OKU Fen Bilimleri Enstitüsü Dergisi
8(2): 856-867, 2025

OKU Journal of The Institute of Science and Technology, 8(2): 856-867, 2025

Osmaniye Korkut Ata Üniversitesi Fen Bilimleri Enstitüsü Dergisi

Osmaniye Korkut Ata University Journal of The Institute of Science and Technology

Enzimatik Sentez Metodu Kullanılarak MWCNT ile Fonksiyonelleştirilen 2-Aminofluoren Tabanlı Malzemeler ve Organik Güneş Hücrelerine Uygulamaları

Betül CANIMKURBEY[1*], Recep TAŞ[2], Melek GÜL[3*]

[1] Ankara Hacı Bayram Veli Üniversitesi, Polatlı Fen Edebiyat Fakültesi, Fizik Bölümü, 06900, Ankara
[2] Bartın Üniversitesi, Fen Fakültesi, Biyoteknoloji Bölümü, 74100, Bartın
[3] Amasya Üniversitesi, Polatlı Fen Edebiyat Fakültesi, Fizik Bölümü, 05100, Amasya

[1]https://orcid.org/0000-0002-6102-5709
[2]https://orcid.org/0000-0002-3743-7770
[3]https://orcid.org/0000-0002-0037-1202
*Sorumlu yazar: bcanimkurbey@gmail.com; melek.gul@amasya.edu.tr

Araştırma Makalesi

Makale Tarihçesi:
Geliş tarihi: 21.11.2024
Kabul tarihi:20.02.2025
Online Yayınlanma: 12.03.2025

Anahtar Kelimeler:
2-Aminofloren
Organic güneş hücreleri
Çok duvarlı karbon nanotüpler
Enzimatik sentez
Döngüsel voltammetri

ÖZ

Bu araştırma, organik güneş hücrelerinde (OSC'ler) potansiyel uygulamaları için 2-aminofluoren (PAF) bazlı bileşiklerin sentezi ve karakterizasyonuna odaklanmaktadır. PAF matrisinin yapısal, elektriksel, kimyasal ve optik özelliklerini değiştirmek ve geliştirmek için çeşitli konsantrasyonlarda çok duvarlı karbon nanotüpleri (MWCNT) içeren PAF sentezine yönelik yeni bir enzimatik yaklaşım önermektedir. Elde edilen modifiye bileşikler daha sonra OSC cihazlarının aktif katmanına dahil edildi. Taramalı elektron mikroskobu (SEM), UV-Vis spektroskopisi, döngüsel voltametri (CV) ve termal analiz dahil olmak üzere kapsamlı karakterizasyon teknikleri, MWCNT dahil edilmesinin etkilerini değerlendirmek için kullanılmıştır. Özellikle, diferansiyel taramalı kalorimetri (DSC) analizi, PAF3'ün 155,60 °C'de en yüksek erime noktasını (T_m) gösterirken, PAF1'in 26,14 °C'de en yüksek cam geçiş sıcaklığını (T_g) gösterdiğini ortaya koymuş ve bu da bu malzemeler için olumlu termal kararlılık ve işleme özelliklerini göstermiştir. Ek olarak, enerji boşluğunun (Egap) PAF3 için 5,51 eV'de en düşük olduğu bulunmuştur; PAF1'in E_{gap}'ı 7,65 eV idi ve bu da PAF3 için iyileştirilmiş yük taşıma özelliklerini önerilmiştir. Sonuçlar, OSC'lerin fotovoltaik performans parametrelerinde önemli iyileştirmeler göstererek, MWCNT'lerin güneş enerjisi uygulamaları için PAF bazlı malzemelerin özelliklerini optimize etmedeki yararlı rolünü vurgulamıştır.

Enzymatic Synthesis and Functionalization of 2-Aminofluorene-Based Compounds with Multi-Walled Carbon Nanotubes (MWCNT) for Enhanced Performance in Organic Solar Cells

Research Article

Article History:
Received: 21.11.2024
Accepted: 20.02.2025
Published online: 12.03.2025

Keywords:
2-Aminofluorene
Organic solar cells
Multi-walled carbon nanotubes
Enzymatic synthesis
Cyclic voltammetry

ABSTRACT

This research focuses on the synthesis and characterization of 2-Aminofluorene (PAF)-based compounds for their potential application in organic solar cells (OSCs). We present a novel enzymatic approach to the synthesis of PAF, which incorporates multi-walled carbon nanotubes (MWCNT) at varying concentrations to modify and enhance the structural, electrical, chemical, and optical properties of the PAF matrix. The resultant modified compounds were subsequently incorporated into the active layer of OSC devices. Comprehensive characterization techniques, including scanning electron microscopy (SEM), UV-Vis spectroscopy, cyclic voltammetry (CV), and thermal analysis, were employed to evaluate the effects of MWCNT incorporation. Notably, differential scanning calorimetry (DSC) analysis

revealed that PAF3 exhibited the highest melting point (T_m) at 155.60 °C, while PAF1 demonstrated the highest glass transition temperature (T_g) at 26.14 °C, indicating favorable thermal stability and processing characteristics for these materials. Additionally, the energy gap (E_{gap}) was found to be lowest for PAF3 at 5.51 eV, compared to PAF1, which exhibited an Egap of 7.65 eV, suggesting improved charge transport properties for PAF3. The results demonstrated significant enhancements in the photovoltaic performance parameters of the OSCs, underscoring the beneficial role of MWCNTs in optimizing the properties of PAF-based materials for solar energy applications.

To Cite: Canımkurbey B., Taş R., Gül M. Enzymatic Synthesis and Functionalization of 2-Aminofluorene-Based Compounds with Multi-Walled Carbon Nanotubes (MWCNT) for Enhanced Performance in Organic Solar Cells. Osmaniye Korkut Ata Üniversitesi Fen Bilimleri Enstitüsü Dergisi 2025; 8(2): 856-867.

1. Introduction

Due to their low cost, adaptable structure, and the lightweight and flexible nature of their modules, organic solar cell (OSC) devices have seen rapid development (Del et al., 2010). In OSCs, which are formed by laying down organic semiconductors between electrodes, the utilize of semiconductors as active layers has notably provided to the advancement of OSCs. This is largely because of the variety and versatility of polymers, their applicability over broad and flexible surfaces, ease of production, and quick processing methods (MacDiarmid and Heeger 1980; Gerard et al., 2002; Winder and Sariciftci 2004; Sonmez et al., 2005).

Since the charge diffusion capacity in polymers is limited, the photon-absorbing active layer in OSC devices requires a homogeneous donor-acceptor structure to facilitate efficient charge separation. When photons reach the polymer layer of the OSC's active layer, excitons are generated, which then separate into electrons and holes in the presence of an electric field from the electrodes. Electrons collect at the anode, while holes accumulate at the cathode, resulting in an electrical current generated from this charge transfer process (Meissner et al., 1992; Sariciftci et al., 1993; Schilinsky et al., 2002; Gregg and Hanna 2003; Spanggaard and Krebs 2004). Transparent conductive polymers have been investigated to facilitate charge transfer in OSC devices (Tian et al., 2004).

Polymers generally exhibit good solubility in solutions. In this work, the layers of OSCs were prepared using the spin-coating technique, while the aluminum electrode were deposited via thermal evaporation, as these methods are both economical and efficient (Parker 1994; Mattox 1998; Hadziioannou and Malliaras, 2006).

Poly(2-aminofluorene) (PAF), as a conjugated polymer, attracts attention with its optoelectronic properties and applications. Enzymatic methods are generally preferred in the synthesis of PAF, especially the oxidative polymerization method using horseradish peroxidase (HRP) enzyme is common. This method increases the reaction rate, minimizes the formation of by-products and provides high purity polymer. The optical band gap of PAF is typically around 2.6 eV, and its fluorescence properties can vary depending on the type of solvent, allowing the material to be used in a variety of electronic applications (Wei et al., 2020).

The HOMO-LUMO energy levels can be adjusted to desired values by synthesizing various organic molecules (Balzani, 2001). Charge efficiency along the polymer semiconductor chain is executed through the delocalization of π-electrons (Benigni, 2005). Polyfluorenes are unique conjugated polymers known for their low operating voltages and high efficiency. Modifications in polymer processability are enabled by the methylene bridge in the fluorene structure. Alkyl chains attached to the C9 position increase the polymer's solubility in various organic solvents without disrupting π-bond delocalization, thereby enhancing processability (Inaoka and Advincula, 2002).

The integration of conjugated polymers and carbon nanotubes to enhance the performance of organic solar cells (OSCs) has been extensively investigated in the literature. However, the majority of these studies have relied on conventional chemical synthesis methods, which often present challenges related to environmental sustainability and the attainment of high-purity materials. In particular, research on the enzymatic synthesis of 2-aminofluorene-based materials remains scarce, and the potential synergistic effects of multi-walled carbon nanotubes (MWCNTs) in OSC applications have yet to be thoroughly explored.

This study presents the enzymatic synthesis of 2-aminofluorene derivatives, achieving high purity and minimal by-product formation, followed by their integration with MWCNTs to optimize optical, thermal, and electrochemical properties. By employing an environmentally sustainable approach, this work makes a significant contribution to enhancing the efficiency of OSCs. Furthermore, it addresses the gap in the literature regarding enzymatic synthesis and provides novel insights into the integration of 2-aminofluorene-based materials with nanostructures, advancing the field of OSC materials design and development. Multi-walled carbon nanotubes were mixed to the poly(2-aminofluorene) synthesis, as they exhibit semiconductor behavior that enhances electrical conductivity and improve crystallinity of the active layer, thereby strengthening the composites (White et al., 1993; Dekker 1999; Martel et al., 2001; Jun et al., 2012). The enzymatic method was chosen for synthesis due to its accelerated reaction rate and absence of by-product formation after synthesis completion.

2. Materials and Methods

A mixture containing specific ratios of 2-aminofluorene, horseradish peroxidase enzyme, and sodium phosphate buffer in 1,4-dioxane was prepared, to which H_2O_2 was gradually added over a three-hour period while continuously stirring the solution. The resulting polymer was then filtered, washed, and vacuum-dried, completing the enzymatic synthesis of PAF. Subsequently, multi-walled carbon nanotubes (MWCNT) were dispersed in 1,4-dioxane using ultrasonic treatment for 30 minutes to ensure homogeneous dispersion and prevent agglomeration. The dispersed MWCNT solutions were then added to the PAF matrix in varying mass ratios (0.5:1, 1:1, and 2:1) under continuous stirring. The mixtures were stirred at 500 rpm for 2 hours to promote uniform distribution and interaction between the MWCNT and PAF. Finally, the composite materials were filtered, washed with deionized water, and vacuum-dried at 50 °C, resulting in three additional polymer variants, as indicated in Table 1.

A systematic methodology was employed to determine the optimal concentrations of multi-walled carbon nanotubes (MWCNTs) to enhance the optical, electrical, and thermal properties of the active layer materials in organic solar cells (OSCs). MWCNTs are renowned for their high surface area and exceptional electrical conductivity. By introducing MWCNTs at controlled ratios, the study aimed to improve the efficiency of electron transport pathways within the polymer matrix. Notably, lower concentrations of MWCNTs were strategically utilized to achieve a balance between conductivity enhancement and the mitigation of potential issues such as phase separation and agglomeration, which are commonly associated with excessive MWCNT loading.

Table 1. Sample codes created by mixing varying mass ratios of MWCNT to the polymer synthesized via enzymatic method.

Sample	PAF	MWCNT
PAF1	1	1
PAF2	1	2
PAF3	1	0,5

For OSC device fabrication, the ITO-coated glass substrates were sequentially cleaned in ultrasonicator with acetone, deionized water, and ethanol, then desiccated with N_2 gas. To further clean the ITO surface, all substrates were treated with ozone plasma for 5 minutes. Following this treatment, the hole transport layer, poly (styrenesulfonate) (PEDOT: PSS), was spin-coated at 2000 rpm for 60 seconds, then annealed at 120 °C for 20 minutes. Using the identical methods, a poly(3-hexylthiophene) (P3HT)/1-(3-methoxycarbonyl) propyl-1-phenyl[6,6]C_{61} (PCBM)/PAF solution in a 1:1:0.5 ratio in dichlorobenzene was prepared and annealed at 110 °C for 10 minutes. Lastly, using a shadow mask, a 100 nm thick aluminum (Al) cathode was thermally evaporated onto the final layer of the OSC device. The same fabrication process, including layer composition and material ratios, was applied to PAF1, PAF2, and PAF3 samples as active layers, resulting in the formation of three additional OSC devices with different active layers.

3. Results and Discussions

The UV-VIS analyses of the synthesized samples were conducted using a UV-VIS spectrophotometer. For this analysis, four polar solvents dichloromethane (DCM), acetonitrile (ACN), acetone, and dimethylformamide (DMF) were selected to prepare the samples. The excitation and emission spectrum of the PAFs were also recorded in these solvents. Figure 3 displays the UV analysis graphs obtained using (a) DCM, (b) ACN, (c) acetone, and (d) DMF as solvents.

According to the UV analysis graphs, the maximum absorbance of the compounds occurs below the visible region (Figure 1). Among the solutions prepared with different solvents, the highest absorbance, observed within the 200-400 nm range, belongs to the PAF sample prepared with DCM (a). When

considering all samples, it was noted that the absorbance of the solutions prepared with ACN (b) was higher than that observed with other solvents.

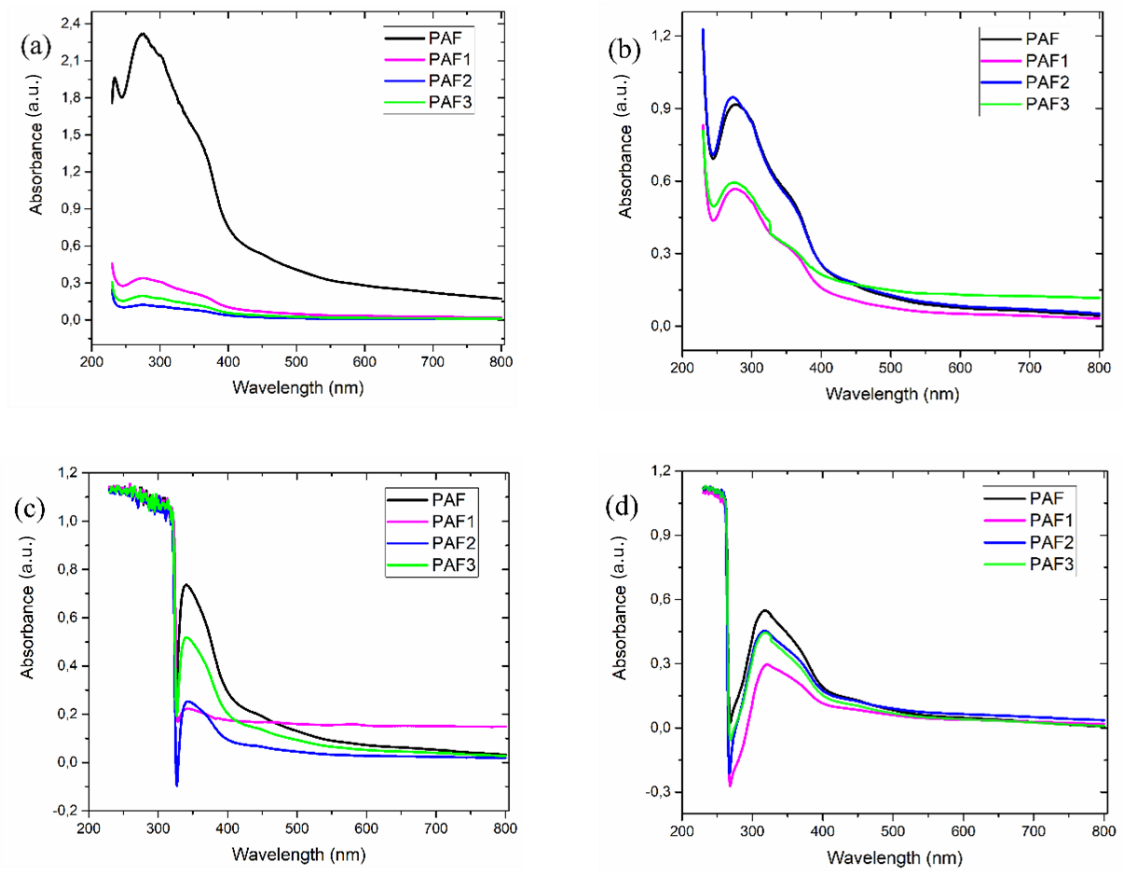

Figure 1. Absorption spectra of the samples formulated in (a) DCM, (b) ACN, (c) acetone, and (d) DMF solutions.

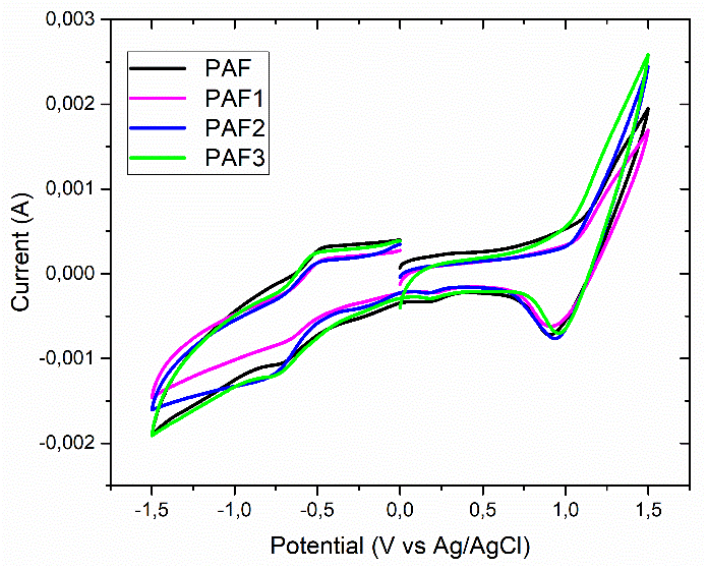

Figure 2. Cyclic voltammetry (CV) analysis graphs of samples.

The Cyclic Voltammetry (CV) analysis of the synthesized samples was performed. A glassy carbon, Ag/AgCl and platinum was used as the working electrode, the counter electrode and the reference electrode, respectively. The solutions were put together in DMF containing TBAP, with compound concentrations at 5 x 10^{-5} M and a sample concentration of 40 ppm. Scanning was conducted over a range of -1.5V to +1.5V at a rate of 10 mV/s, and the resulting distributions for the samples are presented in Figure 2.

According to the CV analysis graph in Figure 2, the anodic peak shifts toward the positive potential, while the cathodic peak shifts toward the negative potential, indicating that the synthesized compounds exhibit electrochemical stability. By determining the oxidation (E_{ox}) and reduction (E_{red}) values from the voltammograms, the E_{gap}, HOMO, and LUMO values were calculated using the equations below and are presented in Table 2 (Cowan and Drisko 1970). Variations in the HOMO-LUMO levels and optical band gaps, as shown in Table 2, are attributed to the different substituted alkyl chains.

$$\mathrm{E(HOMO)} = -\mathrm{e}[E_{ox}^{onset} + 4.4] \quad (1)$$

$$\mathrm{E(LUMO)} = -\mathrm{e}[E_{red}^{onset} + 4.4], \quad (2)$$

Table 2. CV analysis results for the samples.

Sample	E_{ox} (V)	E_{red}(V)	HOMO (eV)	LUMO (eV)	E_{gap} (eV)
PAF	3.11	-7.17	7.61	-2.67	10.28
PAF1	1.56	-6.09	6.06	-1.59	7.65
PAF2	1.49	-7.61	5.99	-3.11	9.10
PAF3	2.52	-2.99	7.02	1.51	5.51

The thermogravimetric (TG), differential thermal analysis (DTA), and derivative thermogravimetry (DTG) graphs of the synthesized samples are presented in Figure 3 for samples.

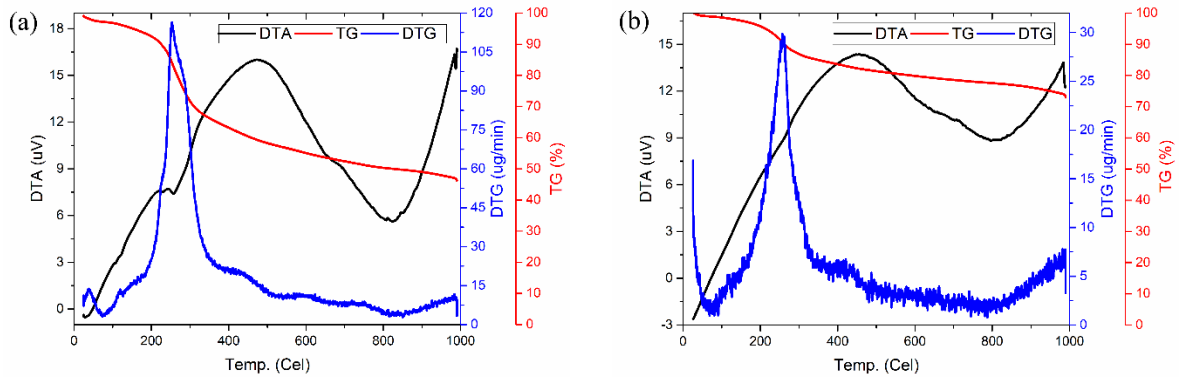

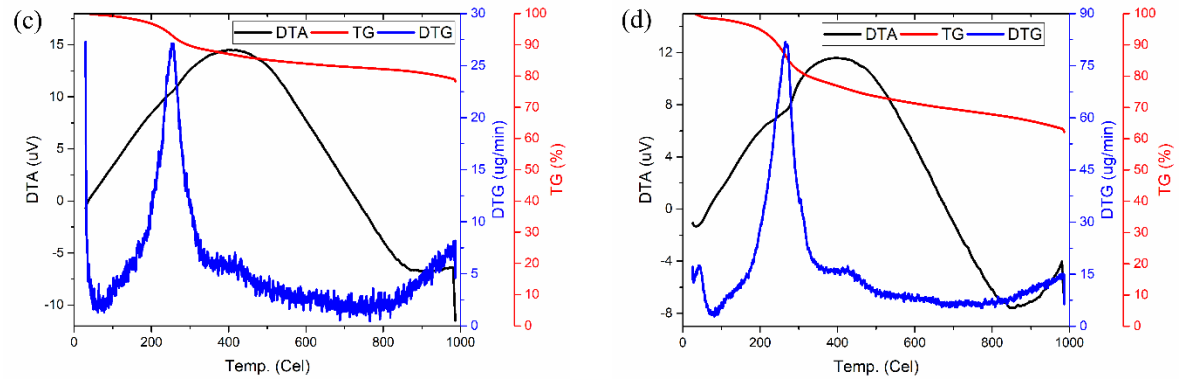

Figure 3. DTA, TG, and DTG thermal analysis graphs of (a) PAF, (b) PAF1, (c) PAF2, and (d) PAF3 samples.

Differential scanning calorimetry (DSC) analyses were performed to determine the thermal properties of the synthesized samples, and DSC graphs for samples are shown in Figure 4. According to Table 4, the maximum mass loss of the samples consist of two stages: the first decomposition is between 200-229 °C, while the second stage ranges between 653-906 °C. The thermal analysis results indicate that due to polymer morphology, the decomposition temperatures in the second stage are higher for the synthesized PAF1, PAF2, and PAF3 samples. The values determined by DTG provide insights into the material's glass transition temperatures, which range from 254-268 °C.

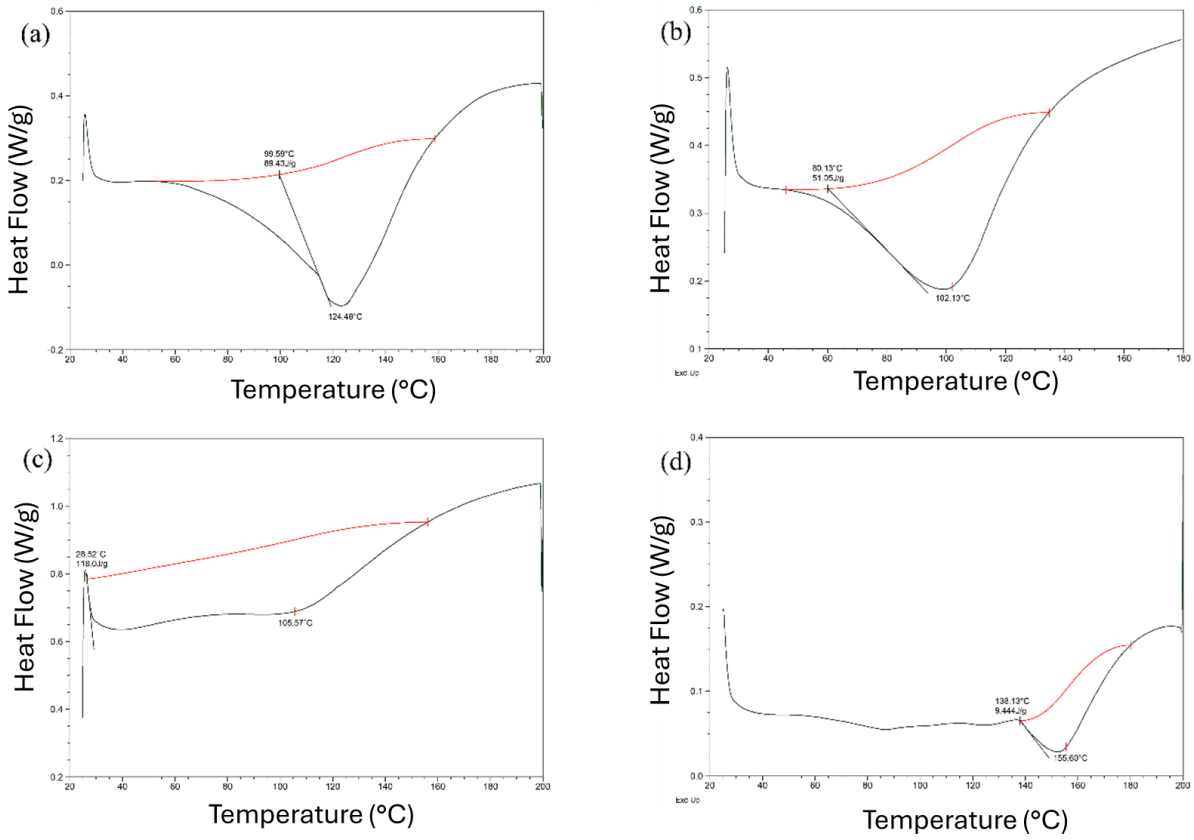

Figure 4. DSC graphs for (a) PAF, (b) PAF1, (c) PAF2, and (d) PAF3 samples.

Table 3. Decomposition, melting, and glass transition temperatures (T_g) for the synthesized samples.

Sample	T_g degree of bonded decomposition	DTG	DSC (Melting Point)	DSC (Glass Transition Temperature)
PAF	229,8-653,3	254.14	124,48	25,59
PAF1	208,8-906,3	261,671	102,13	26,14
PAF2	200,8-911,9	265,91	105,57	25,91
PAF3	219,9-939,0	268,50	155,60	25,34

Based on the thermal analysis shown in Figure 3 and the DSC graphs in Figure 4, the decomposition temperatures, mass losses, and glass transition temperatures (T_g) of the samples are provided in Table 3.

X-ray diffraction (XRD) spectral analyses were performed on the synthesized samples, and the spectra for (a) PAF1, (b) PAF2, and (c) PAF3 are shown in Figure 5.

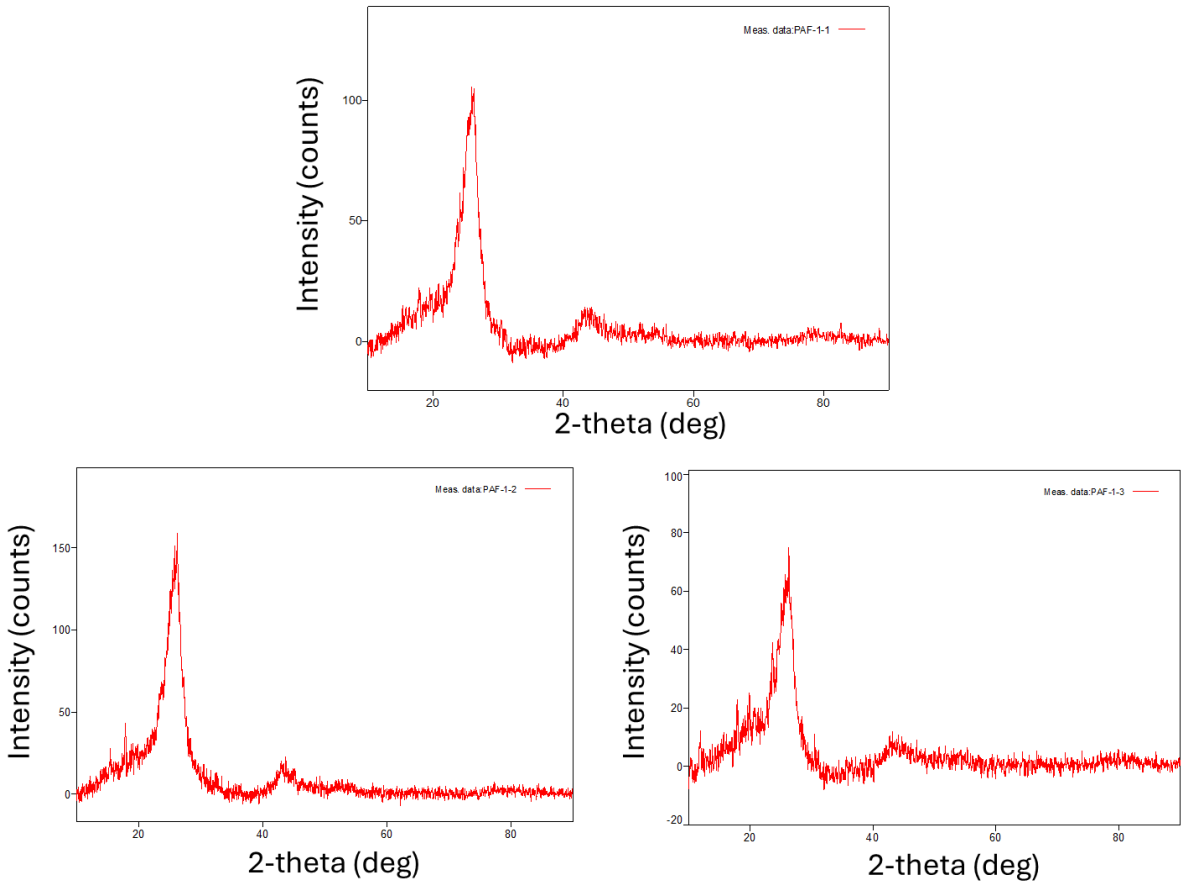

Figure 5. XRD spectrum graph of the samples (a) PAF1, (b) PAF2, and (c) PAF3.

The SEM images of the synthesized PAF sample at (a) 2 µm and (b) 10 µm scales are shown in Figure 6. SEM images obtained for PAF composites provide important information about the material surface

morphology. In the images, it is observed that PAF exhibits a smooth, homogeneous and dense structure. This structure can be explained as a result of the conjugated network structure formed during polymerization and is consistent with the morphology observed in similar polymers reported in the literature (Bilici et al. 2010). The presence of MWCNTs improves the light absorption capacity and electrical conductivity by increasing the surface area. Similar studies in the literature have also stated that carbon nanotube addition significantly increases the mechanical and electrical properties of the polymer matrix (Martel et al., 2001).

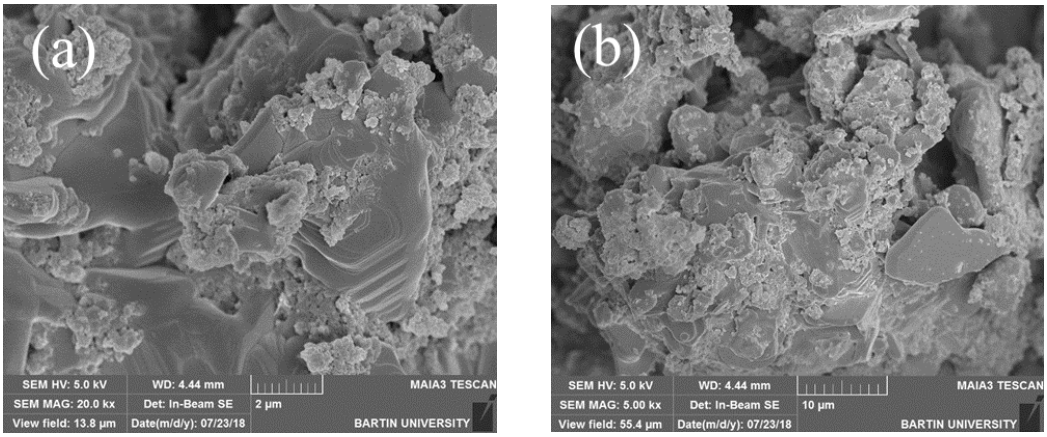

Figure 6. SEM images of the PAF sample at (a) 2 µm and (b) 10 µm scales.

At 25 °C, under the spectral intensity of AM 1.5 sunlight, Figure 7 shows the J-V curves for the OSC devices fabricated with samples.

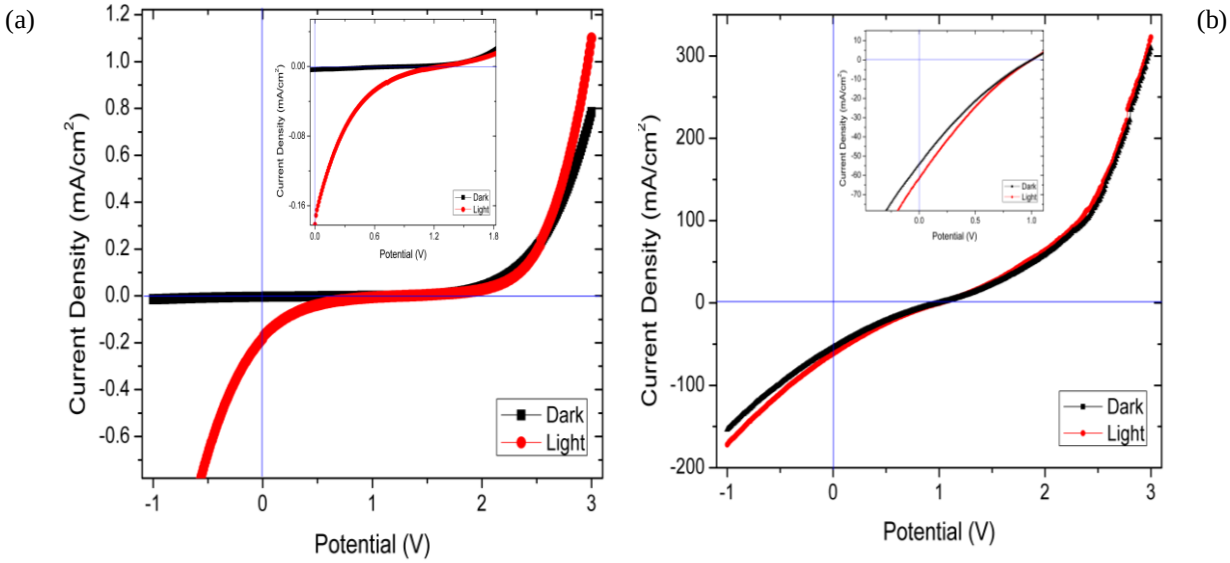

Figure 7. J-V curves of OSC devices fabricated with samples (a) PAF and (b) PAF3.

The values of J_{mpp}, J_{sc}, V_{mpp}, and V_{oc} identified from the graphs in Figure 7 are used to calculate the efficiency (η) and fill factor (FF) of the OSC devices, as presented in Table 4 (Kymakis et al., 2008).

$$FF = \frac{J_{mpp}V_{mpp}}{J_{sc}V_{oc}}, \quad (3)$$

$$\eta = \% \frac{J_{sc}\, V_{oc}\, FF}{P_S}, \quad (4)$$

Table 4. The solar cell parameters for the synthesized samples.

Sample	J_{sc} (mA/cm^2)	V_{oc} (V)	FF (%)
PAF	0.22	1.25	36
PAF3	65	0.92	12

4. Conclusion

This study successfully synthesized and functionalized PAF with varying concentrations of MWCNTs, demonstrating that MWCNT integration enhances the stability and performance of PAF in OSC applications. The improved optical absorption, electrochemical stability, and thermal resilience highlight the potential of these MWCNT-functionalized PAF compounds for use as active layers in organic photovoltaic devices. This research provides a foundation for further exploration into enzyme-catalyzed polymer synthesis as a sustainable method for advanced OSC material development. The enzyme-catalyzed synthesis approach utilized in this study not only facilitated efficient polymerization with minimal by-product formation but also demonstrated the viability of a green chemistry pathway for producing advanced conjugated polymers. Overall, this research lays a strong foundation for future exploration of enzyme-catalyzed polymer synthesis and suggests potential applications in the broader field of optoelectronic devices. Further studies could explore optimization of MWCNT dispersion and concentration, as well as investigate the integration of other nanomaterials to tailor the properties of PAF for specific OSC device architectures.

Conflict of Interest Statement

The authors of the article declare that there is no conflict of interest.

Contribution Rate Statement Summary of Researchers

The authors declare that they have contributed equally to the article.

References

Balzani V. Electron transfer in chemistry, Wiley-VCH 2001.

Benigni R. Structure-activity relationship studies of chemical mutagens and carcinogens: mechanistic investigations and prediction approaches. Chemical Reviews 2005; 105(5): 1767-1800.

Bilici A., Kaya I., Yıldırım M. Biosynthesis and characterization of organosoluble conjugated poly (2-aminofluorene) with the pyrazine bridged. Biomacromolecules 2010; 11(10): 2593-2601.

Cowan DO., Drisko RL. Photochemical reactions. IV. Photodimerization of acenaphthylene. Mechanistic studies. Journal of the American Chemical Society 1970; 92(21): 6286-6291.

Dekker C. Carbon nanotubes as molecular quantum wires. Physics Today 1999; 52: 22-30.

Del G., Belcari AN., Bisogni MG., Losa G., Marcatili S., Ambrosi G., Corsi F., Marzocca C., Dalla Betta G., Piemonte C. Advantages and pitfalls of the silicon photomultiplier (SiPM) as photodetector for the next generation of PET scanners. Nuclear Instruments and Methods in Physics Research Section A: Accelerators, Spectrometers, Detectors and Associated Equipment 2010; 617(1-3): 223-226.

Gerard M., Chaubey A., Malhotra BD. Application of conducting polymers to biosensors. Biosensors and Bioelectronics 2002; 17(5): 345-359.

Gregg BA., Hanna MC. Comparing organic to inorganic photovoltaic cells: Theory, experiment, and simulation. Journal of Applied Physics 2003; 93(6): 3605-3614.

Hadziioannou G., Malliaras GG. Semiconducting polymers: chemistry, physics and engineering, John Wiley & Sons 2006.

Inaoka S., Advincula R. Synthesis and Oxidative cross-linking of fluorene-containing polymers to form conjugated network polyfluorenes: Poly (fluoren-9, 9-diyl-a lt-alkan-α, ω-diyl). Macromolecules 2002; 35(7): 2426-2428.

Jun GH., Jin SH., Park SH., Jeon S., Hong SH. Highly dispersed carbon nanotubes in organic media for polymer: fullerene photovoltaic devices. Carbon 2012; 50(1): 40-46.

Kymakis E., Kornilios N., Koudoumas E. Carbon nanotube doping of P3HT: PCBM photovoltaic devices. Journal of Physics D: Applied Physics 2008; 41(16): 165110.

MacDiarmid AG., Heeger AJ.Organic metals and semiconductors: The chemistry of polyacetylene,(CH) x, and its derivatives. Synthetic Metals 1980; 1(2): 101-118.

Martel R., Derycke V., Lavoie C., Appenzeller J., Chan K., Tersoff J., Avouris P. Ambipolar electrical transport in semiconducting single-wall carbon nanotubes. Physical Review Letters 2001; 87(25): 256805.

Mattox D. Handbook of physical vapor deposition (PVD) processing. Noyes Publications 1998.

Meissner D., Siebentritt S., Guenster S. Charge carrier photogeneration in organic solar cells. Optical Materials Technology for Energy Efficiency and Solar Energy Conversion XI: Photovoltaics, Photochemistry, Photoelectrochemistry, SPIE 1992.

Parker ID. Carrier tunneling and device characteristics in polymer light-emitting diodes. Journal of Applied Physics 1994; 75(3): 1656-1666.

Sariciftci NS., Braun D., Zhang C., Srdanov V., Heeger AJ., Stucky G., Wudl F. Semiconducting polymer-buckminsterfullerene heterojunctions: Diodes, photodiodes, and photovoltaic cells. Applied Physics Letters 1993; 62(6): 585-587.

Schilinsky P., Waldauf C., Brabec CJ. Recombination and loss analysis in polythiophene based bulk heterojunction photodetectors. Applied Physics Letters 2002; 81(20): 3885-3887.

Sonmez G., Sonmez H.B., Shen CK., Jost RW., Rubin Y., Wudl F. A processable green polymeric electrochromic. Macromolecules 2005; 38(3): 669-675.

Spanggaard H., Krebs FC. A brief history of the development of organic and polymeric photovoltaics. Solar Energy Materials and Solar Cells 2004; 83(2-3): 125-146.

Tian S., Liu J., Zhu T., Knoll W. Polyaniline/gold nanoparticle multilayer films: assembly, properties, and biological applications. Chemistry of Materials 2004; 16(21): 4103-4108.

Wei W., Liu Z., Liang C., Han GC., Han J., Zhang S. Synthesis, characterization and corrosion inhibition behavior of 2-aminofluorene bis-Schiff bases in circulating cooling water. RSC advances 2020; 10(30): 17816-17828.

White C., Robertson D., Mintmire J. Helical and rotational symmetries of nanoscale graphitic tubules." Physical Review B 1993; 47(9): 5485.

Winder C., Sariciftci NS. Low bandgap polymers for photon harvesting in bulk heterojunction solar cells. Journal of Materials Chemistry 2004; 14(7): 1077-1086.